FULL-LENGTH REPRINT – differs from the original in layout but not in contents
Chmielewski L.J., Bator M., Hough transform for opaque circles measured from outside and fuzzy voting for and against.
In L. Bolc et al., editors, Proc. Int. Conf. ICCVG 2012,
volume 7594 of Lecture Notes in Computer Science, pages 313-320, Warsaw, Poland, 24-26 Sep 2012.
 doi:10.1007/978-3-642-33564-8_38
The original publication is available at http://www.springerlink.com .
Contains erratum – see crossed coloured text and margin notes

Hough Transform for Opaque Circles Measured from Outside and Fuzzy Voting For and Against*

Leszek J. Chmielewski and Marcin Bator

Warsaw University of Life Sciences (SGGW),
Faculty of Applied Informatics and Mathematics
{leszek_chmielewski,marcin_bator}@sggw.pl, http://wzim.sggw.pl

Abstract. Geometrical limitations on the voting process in the classical Hough transform resulting from that the detected objects are opaque to the applied means of measurement are considered. It is assumed that the measurements are made from one point, like in LIDAR scanning. The detected object is a circle and the two point elementary voting set forming its chord is considered. The first type of conditions are those which can be used during the accumulation process. The *side condition* says that the circle lies at the opposite side of the chord than the laser source. The *magnitude condition* requires that points in the elementary set must not be occluded with respect to the source by any circle hypothesised in voting. The second type of conditions can be checked after after the detection. They require that points are neither inside the object nor in its shadow. Departures from this rule are admitted, so fuzzy voting between positive and negative evidence for the object is considered.

Keywords: Hough transform, opaque circles, negative evidence, LIDAR

1 Introduction

Hough transform (HT) is one of the oldest methods of robust detection of objects [2]. Although a lot has been said on occlusions in images (e.g. [6]), it seems that little or no attention has been paid to the geometrical limitations on the evidence accumulation process coming from that the detected object can be opaque to the means which forms the measuring points. Special cases are radar and LIDAR detectors. Without losing generality, let us concentrate on LIDAR (LIght Detection And Ranging) measurements. One of the applications of LIDAR are measurements of forest and trees being the subject of intensive investigations (cf. [5]). Similar measurements are made for example on architectural objects.

The result of LIDAR measurements is a cloud of points being a sparse image in which direct differentiation is impossible. Therefore, from the many versions of HT we chose that with the elementary voting set formed by two points (see e.g. [4], Section 5.4.5.2).

In this paper our target is to present the conditions which constitute a theoretical result rather than their influence on the quality of specific measurements belonging to some chosen class. However, selected real-world results will be shown to exemplify the considerations.

* L. Bolc et al. (Eds.): ICCVG 2012. LNCS 7594, pp. 313-320, 2012.

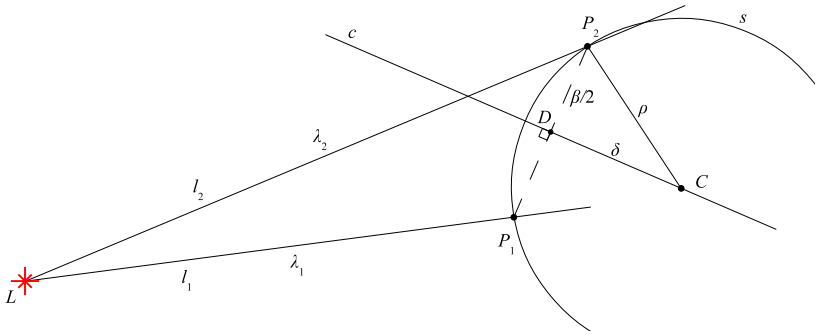

Fig. 1. Geometry for the circle detection with the Hough transform with a pair of points as an elementary set. See text.

2 Basic geometry

The points will be denoted by uppercase Roman letters; lines, line segments, circles and arcs – by lowercase Roman letters, and distances – by Greek letters.

The laser light source or the viewpoint is L, as shown in Fig. 1. To form one vote two measuring points are taken into account: P_1 and P_2, where P_2 is the farther from the source L. A point P_j has its intensity I_j. As the intensity of the pair to be used in the accumulation the intensity of the weaker point will be taken. Let us call $\overline{P_1P_2}$ the base. The lines connecting the source with the measuring points are l_1 and l_2, and the respective distances are λ_1 and λ_2. The distance between points is β (base distance). The circles for which these two points can vote have to pass through them, so their centres must lie on c which is the midperpendicular of $\overline{P_1P_2}$. Let D be the middle of $\overline{P_1P_2}$.

In Fig. 1 a possible circle s is shown with the centre C lying at the distance δ from D, and with radius ρ. Usually in HT a range of possible radii is assumed, $\rho \in [\rho_{m'}, \rho_x]$. Subscripts m' and x denote minimum and maximum, respectively. As the locus of possible circle centres the points on c at the distance $\delta \in [\delta_{m'}, \delta_x]$ to D should be considered:

$$\delta_{m'}^2 + (\beta/2)^2 = \rho_{m'}^2 \ , \quad \delta_x^2 + (\beta/2)^2 = \rho_x^2 \ . \tag{1}$$

In the classical HT this is basically all what is done to limit the range of locations of centres on the line c. Now we shall pass on to the new conditions which result from that the circular object is opaque and the measurement points are all visible from the source of measuring rays.

3 Conditions

The conditions which follow from the geometry of the problem can be divided into two types. The first type are those conditions which can be checked using only the knowledge on the viewpoint and the currently considered measuring points. These conditions can be checked during the accumulation. They influence

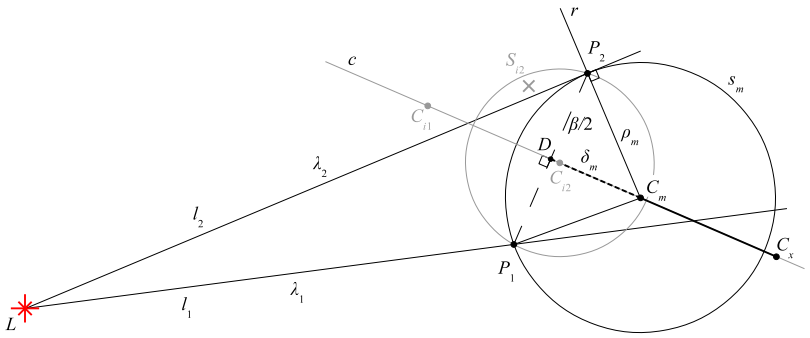

Fig. 2. Geometry for conditions checked during accumulation. Minimum possible circle $s_m(C_m, \rho_m)$ (black) and impossible circle s_{i2} (grey). See text.

the accumulator contents and in this way they improve the quality of detection results during the process of their formation. The second type are the conditions for which it is necessary to have the information on the detected circles and on some or all the measuring points. These conditions can be used to check the consistence and possibly to correct the results after they have been received.

3.1 During the accumulation

Condition of side We shall use some more notations shown in Fig. 2.

The first, basic observation is that the circle must be behind rather than in front of the base $\overline{P_1P_2}$ with respect to the source L:

$$\overrightarrow{LD} \circ \overrightarrow{DC} > 0 \,. \tag{2}$$

The centre C_{i1} is on the wrong side of the base and hence it is impossible. To visualise this condition the part of c at the left from D has been marked grey.

This simple observation eliminates the false detection of concave objects as circles (see Fig. 4a1–b2, Section 4).

Condition of magnitude It can be seen in Fig. 2 that the circle s_{i2} which satisfies the condition of shades the point P_2 from the light source L. The circle segment which protrudes above l_2 marked with a grey slanted cross is impossible, so the whole circle is impossible due to that it is too small. There exists a minimum radius ρ_m for which the shading phenomenon does not take place. The minimum circle $s_m(C_m, \rho_m)$ is tangent to l_2 going from L to the farther measuring point P_2, so r passing through P_2 and C_m is normal to l_2. Note that the location of C_m and the lengths ρ_m, δ_m are different from those marked with m' in (1). Finally, the more restrictive values should be taken. The locus of impossible circle centres at the right-hand side of D, has been marked with a thick broken line.

Now, the equations are

$$2\,\overrightarrow{P_1D} = \overrightarrow{P_1P_2} \,, \quad \overrightarrow{LP_2} \circ \overrightarrow{P_2C_m} = 0 \,, \quad \overrightarrow{P_1P_2} \circ \overrightarrow{DC_m} = 0 \,. \tag{3}$$

There are four unknowns: the coordinates of D and C_m. D can be found from the first equation. The set (3) is linear with respect to the coordinates of C_m.

In LIDAR measurements the coordinate system origin is frequently located in L. Denote the coordinates x and y of any point T or projections of any distance τ as x_T, y_T and x_τ, y_τ, respectively. Then, $x_{\lambda_j} = x_{P_j}$, $y_{\lambda_j} = y_{P_j}$, $j = 1, 2$. Also, always $x_\beta = x_{P_2} - x_{P_1}$, $x_D = (x_{P_2} + x_{P_1})/2$, the same for y. Denote plainly $x_{P_j} = x_j$, $y_{P_j} = y_j$, $j = 1, 2$. The solution is

$$\begin{aligned} T &= x_2 y_1 - y_2 x_1 \,, \\ T_{x_{C_m}} &= [(x_2^2 + y_2^2) - (x_1^2 + y_1^2)]\, y_2/2 \;-\; (x_2^2 + y_2^2)(y_2 - y_1) \,, \\ T_{y_{C_m}} &= (x_2^2 + y_2^2)(x_2 - x_1) \;-\; [(x_2^2 + y_2^2) - (x_1^2 + y_1^2)]\, x_2/2 \,. \end{aligned} \tag{4}$$

$$x_{C_m} = T_{x_{C_m}}/T \,, \quad y_{C_m} = T_{y_{C_m}}/T \,. \tag{5}$$

The main determinant T is not zero as long as P_1 does not belong to l_2, which is compatible with the visibility condition. Now it is easy to find the minimum distance $\delta_m = |\overrightarrow{DC_m}|$ and radius $\rho_m = |\overrightarrow{P_2C_m}|$.

The locus of possible circle centres is marked in Fig. 2 with a thick black line from C_m just found to C_x at the distance δ_x from D in the direction out from L, found as previously from (1).

An example of a positive influence of the condition of magnitude on the detection result can be seen in ~~Fig. 4a and c~~ in Section 4.

It should be: Fig. 4.1 and 4.3

Both conditions are relatively simple to calculate and their complexity is linear with respect to the calculations routinely made in the Hough transform.

3.2 After the detection

The measurement points should be on the surface S of the detected object. They can also be outside, but neither inside the object nor in its shadow, with respect to L. The points on the surface which gave rise to a maximum in the Hough accumulator pertaining to the object constitute the positive evidence for its existence ~~E_+~~. The points inside and in the shadow constitute negative evidence ~~E_-~~. ~~Both $E_- \leq 0$~~. Due to practical reasons some negative evidence can be admitted as long as it is much smaller than the positive one. What this means should be defined according to the domain at hand. A reasonable simple condition could be linear:

E^+

E^-. Both $E^\pm \geq 0$.

$$\text{~~}\kappa\, E_+ > E_-\text{~~} \,, \quad \kappa \in (0, 1) \,. \tag{6}$$

$\kappa\, E^+ > E^-$

If a point can be inside the object to some extent, then it should be acceptable for it to be in the shadow to the corresponding extent. A definition of a fuzzy membership function μ_j for evidence carried by a single point j is necessary. It can be assumed that any of the evidences E^+, E^- is an algebraic sum of evidences of points that constitute it, weighted by their intensities:

$$E^\pm = \sum_j I_j\, \mu_{P_j^\pm} \,, \quad \mu_j \in [0, 1] \,. \tag{7}$$

It is reasonable to assign the membership 1 to any point which constituted a maximum corresponding to the object in the Hough accumulator. To find such points it may be necessary to use the HT with reverse addressing.

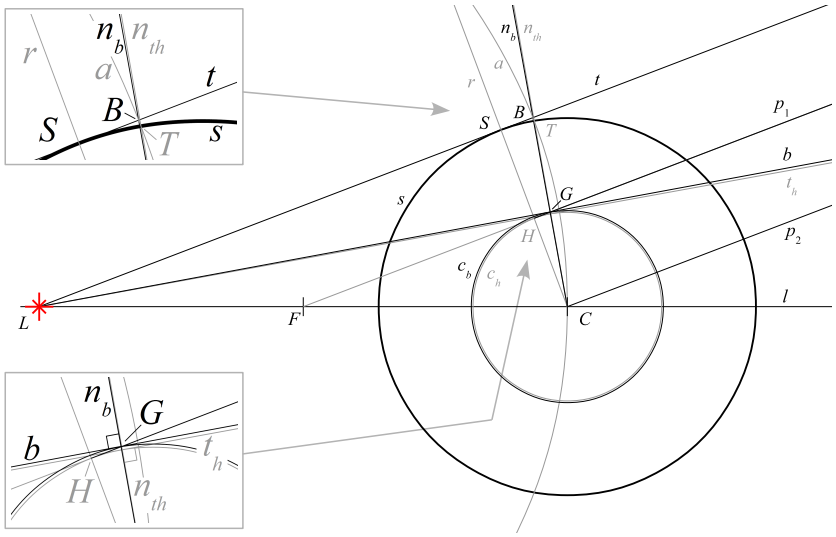

Fig. 3. Geometry for the conditions to be checked after the detection. Grey circle c_H has half radius of the object surface circle s. Its tangent passing through L and normal to tangent passing through C drawn in grey. Objects related to the bisector b of angle CLB and its tangent circle c_b marked in black. Details in the lower part of the image, symmetrical around l, are omitted. See text.

Now let us consider the membership function for the points of negative evidence P_j^-. Let us span the membership function along the radius, from the surface s of the object down to its centre C, so that it is zero at s and one in C (Fig. 3). Assume we wish this function to be liberal towards negative evidence so assign it the value 0.5 at half radius. An example of such a function is

$$\mu(P) = \frac{1}{2}\left(\cos\frac{\pi|\overline{CP}|}{|\overline{CS}|} + 1\right) . \tag{8}$$

It should be: μ_P

This function will hold in the frontal part of the circle, that is, in front of r (and downward, symmetrically). It can be extended to the shadow part in two ways. The first way is to draw lines parallel to the tangent t, first p_1 tangent to circle c_h (with half radius) and second p_2 passing through C. The function (8) can be spanned between t and p_2 with p_1 in the middle, forming a continuation to the right of r of the frontal part of s with c_h in the middle. So, the admissible zone for shadowed points has constant width and is parallel to the tangent t. The second way is related to a postulate that the width of the admissible zone should grow together with the distance from L. A good idea would be to construct it around the bisector b of $\angle CLB$. However, B is tangent to a circle c_b different from c_h. This can be seen by investigating the details of Fig. 3: b divides $\angle CLB$ into halves and it is tangent to c_b, while c_h divides $\overline{CB}$ into halves and is tangent to t_h. T is near but never equal to B (they both lie on arc a). What links c_h to b is a short fragment of p_1 from r to n_b. It is tangent to c_b but forms an angle with b, so the link is only C^0 smooth. Hence, there is a difficulty in making the function like (8) spanned along lines parallel to CB in the shadow smoothly pass

into the function defined on the radius of s in the front. One can easily invent geometrical constructs to overcome this difficulty, but each of them needs some care. If we wish that the point $\mu = 0.5$ were somewhere else than the middle, the above structure changes quantitatively but the geometrical relations remain similar.

It should be:
$\mu. = 0.5$
than in the middle

Checking each detected circle against all the measuring points would be impractical if the total field of view were large, so simplifications are necessary. A simple idea would be to restrict the tests to the near neighbourhood of each circle. Using probabilistic voting schemes would also be a good solution [3].

4 Examples for the problem of detection and measurement of trees

Here we shall try to show the influence of the proposed conditions on detection results for actual measurements. As the examples we shall use the LIDAR images of fragments of a forest. These fragments have been segmented out from larger data with the intention to receive a cross-section of a single tree at the breast height in one image, as described in our previous work [1]. However, due to small diameters of some trees and the presence of clutter (leaves and thin branches), some images contain multiple tree trunks. The classic HT can fail to find only the trunks. The conditions introduced above improve some of the erroneous results.

Conditions checked during accumulation The functioning of these conditions is shown in Fig. 4. The contents of the accumulator shown in image $b1$ is irrational. Moreover, there is a local maximum pertaining to the lower right object, which is concave. The global result a2 is still erroneous, but the maximum coming from the concave object is now cancelled. The condition of side makes the accumulator contents more realistic for the case. After applying the magnitude condition a large number of false votes are dismissed so the largest maximum in image b3 and the result in image a3 are correct.

The parameters used in the accumulation process were: 500 pix/m, minimum circle radius 0, maximum 0.3 m, accumulator fuzzified with the inverted parabolic function in a 5×5 pix window. The layer containing about 700 measurement points projected on the image plane extended for ± 2 cm around the breast height equal to 130 cm above the ground. Data used in this paper can be made available at request.

Conditions checked after the detection In Fig. 5a, a typical example of data points ie inside a circle but are acceptable is shown. In this case a detected tree had a natural hollow or was partly broken. The spurious points are less numerous than those at the surface, so their negative evidence can be considered as weak with respect to the positive evidence. Such images were the rationale for designing the membership function which accepts seemingly false points relatively deep under the front surface of the object. Another cue for accepting some points inside the objects and in their shadows was the dynamic character of a tree which

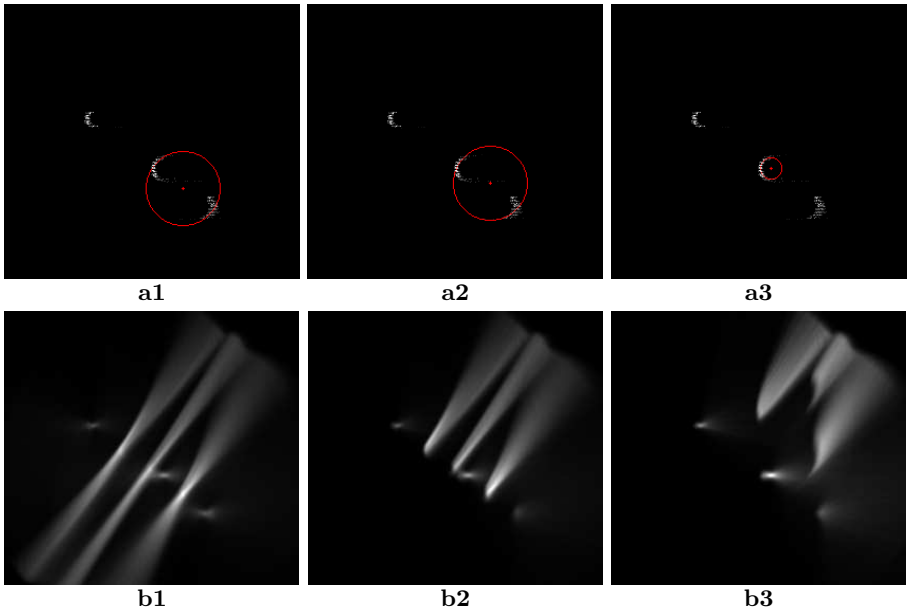

Fig. 4. Example of the influence of conditions checked during accumulation (Section 3.1) on the accumulator and the detection result. (**a**) Data points and the detected strongest circle; (**b**) accumulator. (**1**) Classical HT, no conditions; (**2**) condition of side checked; (**3**) condition of magnitude checked. The laser was at the west, at a relatively large distance with respect to the image size.

can wave in the wind. This is not the case for architectural objects. The example of unacceptable points is in Fig. 5b, where there are less points on the surface than inside the tree.

5 Conclusions and open problems

Two types of conditions necessary in the detection of opaque objects have been proposed. The conditions are implied by that the measuring points indicating the surface of the object have to be visible from the viewpoint of the measuring device. The case of detecting circular objects with the Hough transform has been considered. The proposed conditions of the first type, that is, the conditions of side and magnitude are applied during the accumulation process itself and do not require extensive additional calculations. The conditions of the second type verify the consistence of the detection results with the data and can be checked after the detection is made. The results can be used to modify the Hough accumulator, but the accumulation and checking the condition are separate processes.

The presented study opens a number of new problems. Efficient organisation of the processes of verification after detection and of backtracking to correct the inconsistent results is an interesting open question. Extension to the shapes

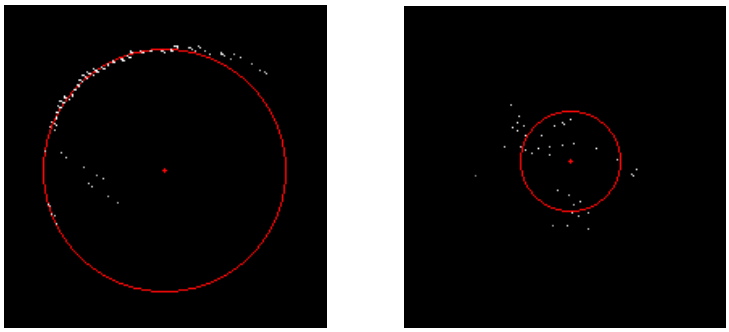

a **b**

Fig. 5. Example for the conditions checked after the detection (Section 3.2) on the accumulator and the detection result. (**a**) good; (**b**) bad. Laser was far at north-west.

other than circles is possible. Verification of various membership functions for creating the sets of positive and negative evidence seems to be the vital next step which should be made in order to improve the quality of measurements as far as practical applications are considered.

Acknowledgements The research has been financed from the budget resources for science in the years 2010-2013 as the project of the Ministry of Science and Higher Education no. N N309 139739.

We wish to thank Krzysztof Stereńczak and Michał Zasada from the Faculty of Forestry, Warsaw University of Life Sciences (SGGW), for valuable discussions and for providing the LIDAR data used in the experiments.

References

1. L.J. Chmielewski, M. Bator, M. Zasada, K. Stereńczak, and P. Strzeliński. Fuzzy Hough transform-based methods for extraction and measurements of single trees in large-volume 3D terrestrial LIDAR data. In volume 6374 of *Lecture Notes in Computer Science*, pages 265–274, 2010. Springer, Heidelberg. doi:10.1007/978-3-642-15910-7_30.
2. P.V.C. Hough. Machine analysis of bubble chamber pictures. In *Proc. Int. Conf. on High Energy Accelerators and Instrumentation*. CERN, 1959.
3. H. Kälviäinen, P. Hirvonen, L. Xu and O. Erkki. Probabilistic and non-probabilistic Hough transforms: overview and comparisons. *Image and Vision Computing*, 13(4):239–252, 1995. doi:10.1016/0262-8856(95)99713-B.
4. M. Nixon and A. Aguado. *Feature Extraction & Image Processing*. Newnes, Oxford, Auckland, Boston, 2002.
5. P. Rönnholm, H. Hyyppä, and J. Hyyppä, editors. *Proc. ISPRS Workshop on Laser Scanning 2007 and SilviLaser 2007*, volume XXXVI, part 3/W52 of *IAPRS*, Espoo, Finland, 12-14 Sep 2007.
6. D. Soukup and I. Bajla. Robust object recognition under partial occlusions using NMF. *Computational Intelligence and Neuroscience*, vol. 2008, Article ID 857453, 14 pages, 2008. doi:10.1155/2008/857453.